香港科技大學
THE HONG KONG UNIVERSITY OF SCIENCE AND TECHNOLOGY

NF-Heart: A Near-field Non-contact Continuous User Authentication System via Ballistocardiogram

Yandao Huang[1,2], Minghui Qiu[2], Lin Chen[2], Zhencan Peng[3], Qian Zhang[1], and Kaishun Wu[2]

1. Hong Kong University of Science and Technology
2. Hong Kong University of Science and Technology (Guangzhou)
3. Shenzhen University

www.yandaohuang.cn

Ubicomp 2023
October 8th-12th

Background

54% Organizations

450% growth in 2020

1 Bil. Records of Attack

$5 Trillion business lost

One-pass Authentication Vs. Continuous Authentication

Existing Continuous Authentication (CA) Methods

1. Behavioral based

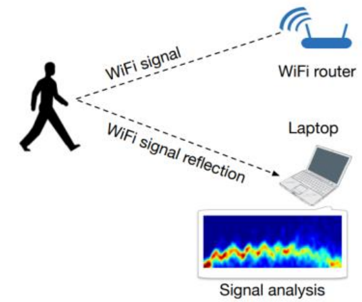

Gait—WiFiU


Keystroke Dynamics

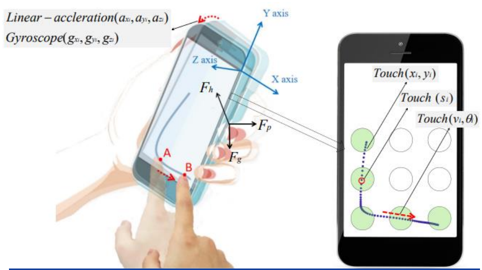

Touch—TouchID


Eye movement

2. Physiological based

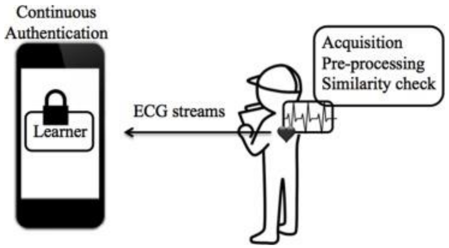

ECG

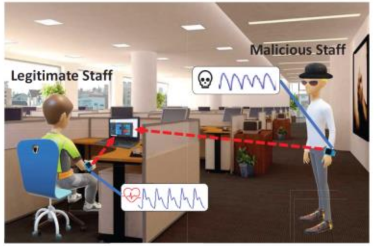

PPG—TrueHeart

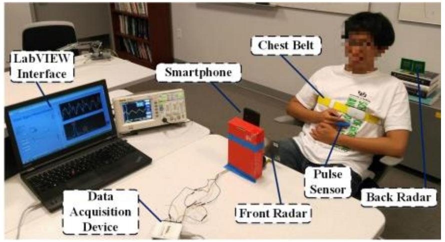

RFG—Cardiac Scan

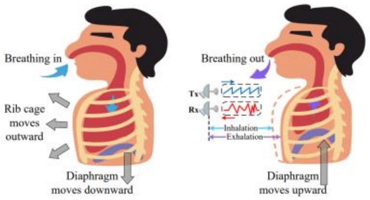

Breath—M-Auth

Our work

80% of working hour sitting

12 h seated

Can we turn a common chair into an automatic identity "scanner"?

NF-Heart: a secure and unobtrusive **continuous authentication (CA)** system based on **near-field non-contact ballistocardiogram (BCG) measurements**

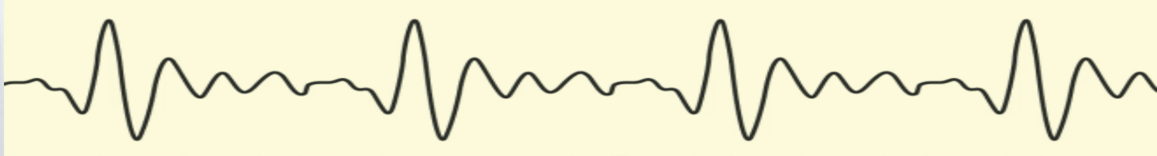

In-home adaptation for IoT device

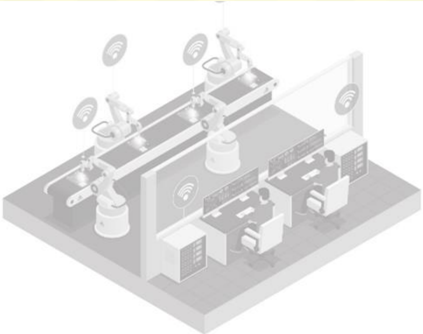

Remote Factory Security & Management

Our work

NF-Heart:

Continuous authentication (CA)

Near-field & Non-contact

Ballistocardiogram (BCG)

In-home adaptation for IoT device

Remote Factory Security & Management

Principle of NF-Heart

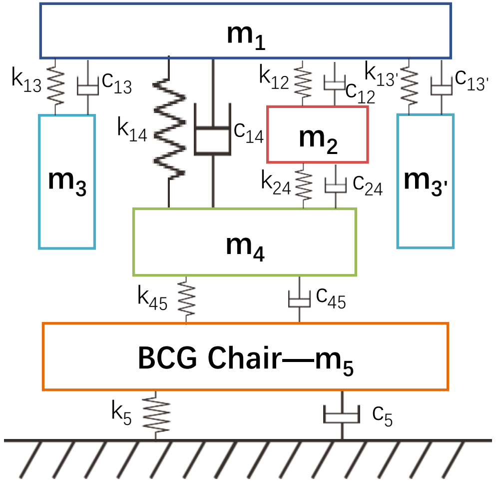

m_1: upper torso

m_2: internal organs

m_3&$m_{3'}$: upper limbs

m_4: lower limbs

m_5: External chair

k: spring coeff.

c: damping coeff.

6-DoF spring-mass-damper model

Key Insights:

1. BCG measures body's **gravity changes** caused by the **recoil force** of the body in reaction to the ejection of blood.
2. BCG transmission from internal blood vessels to the external **body (m, c, k)** can be estimated as an **encryption process** due to non-linear effects.

System Workflow

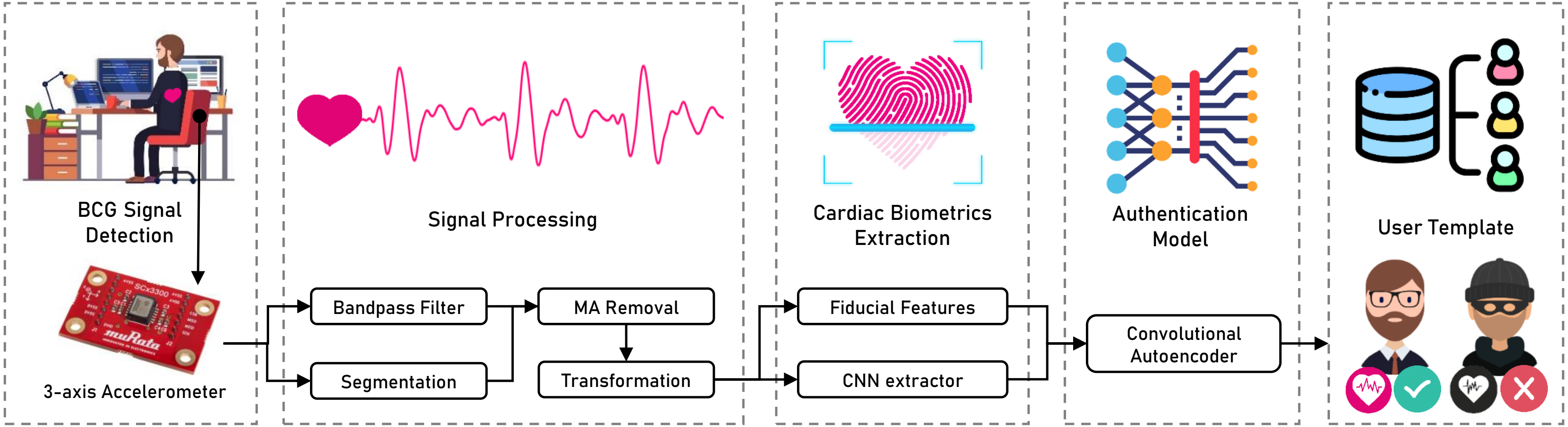

CHALLENGES

1. BCG is sensitive to **motion artifacts (MAs)**
2. The unavoidable **effects of respiration, sitting posture, and user emotion** on BCG signals

SOLUTIONS

1. **Hidden Signal Quality Index (H-SQI)** for MA Detection. A **Two-stage MA-removal** using **CEEMDAN** and **VS-LMS** for MA Removal.
2. We proposed a **BCG dynamic model** with 14 Gaussian Kernels to **transform** the BCG signals

Methodology——Motion Artifact Detection

$$\text{Shape Factor} = \frac{\sqrt{\frac{1}{N}\sum_{i=1}^{N} x_i^2}}{\frac{1}{N}\sum_{i=1}^{N} |x_i|}$$

$$\text{Standard Deviation} = \sqrt{\frac{1}{N}\sum_{i=1}^{N}(x_i - \bar{x})^2}$$

$$\text{Impulse Factor} = \frac{\max(x_i) - \min(x_i)}{\frac{1}{N}\sum_{i=1}^{N} |x_i|}$$

$$\text{Root Mean Square} = \sqrt{\frac{1}{N}\sum_{i=1}^{N} x_i^2}$$

$$\text{Skewness} = \frac{\frac{1}{N}\sum_{i=1}^{N}(x_i - \bar{x})^3}{\left(\frac{1}{N}\sum_{i=1}^{N}(x_i - \bar{x})^2\right)^{\frac{3}{2}}}$$

$$\text{Kurtosis} = \frac{\frac{1}{N}\sum_{i=1}^{N}(x_i - \bar{x})^4}{\left(\frac{1}{N}\sum_{i=1}^{N}(x_i - \bar{x})^2\right)^{2}}$$

$$\text{Clearance Factor} = \frac{\max(x_i) - \min(x_i)}{\left(\frac{1}{N}\sum_{i=1}^{N}\sqrt{|x_i|}\right)^{2}}$$

Hidden Signal Quality Index (H-SQI)

Methodology——Motion Artifact Removal

Sample result of Hidden Signal Quality Index (H-SQI)

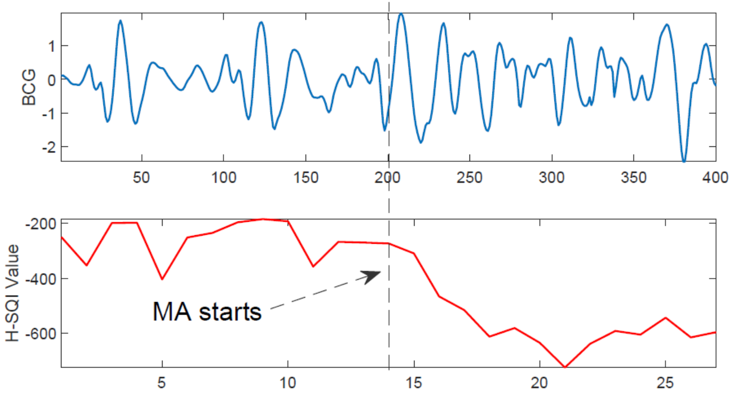

Two-stage Motion Artifact Removal
Stage 1: CEEDAN
Stage 2: VS-LMS

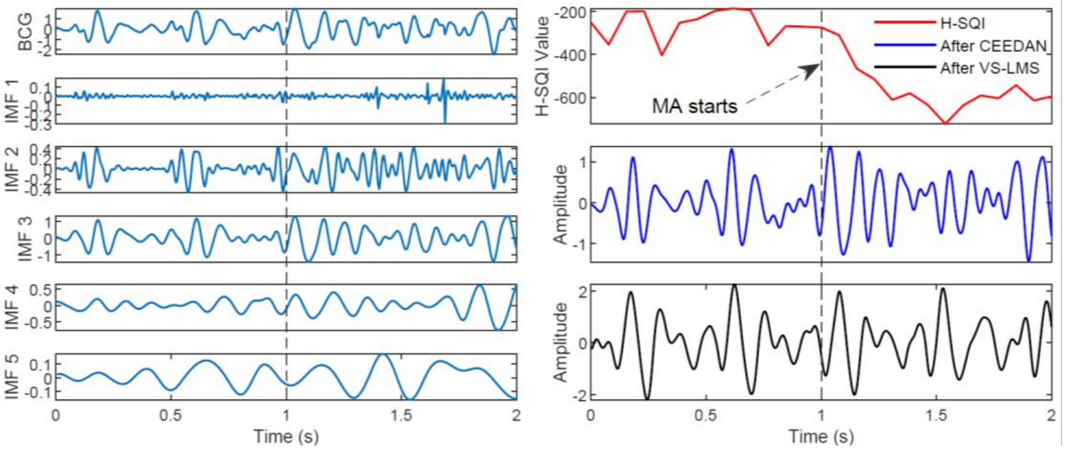

Intrinsic Mode Function **Final Result**

Methodology——Transformation

Challenge 2: BCG dynamical model for eliminating effects of respiration, sitting posture, and user emotion.

$$\begin{cases} \dot{x} = \gamma x - \omega y \\ \dot{y} = \gamma x - \omega y \\ \dot{z} = -\sum_{i \in \{H,I,J,K,L,M,N\}} a_i \Delta\theta_i \exp\left(-\frac{\Delta\theta_i^2}{2b_i^2}\right) - (z - z_0) \end{cases}$$

Integration

Fourth-order Runge–Kutta

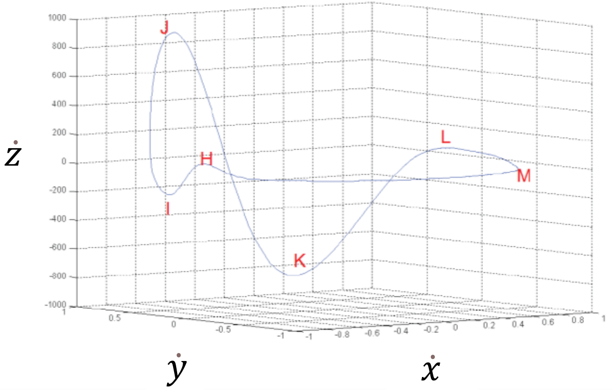

Three-dimensional display of single cycle BCG signals

where

$$\gamma = 1 - \sqrt{x^2 + y^2}$$

ω: angular velocity, related to the beat-to-beat heart rate as $\omega = 2\pi f_1$.

$z_0 = A \sin(2\pi f_2 t)$ The baseline wander of a BCG caused by respiration

We proposed the **BCG dynamical model** for transformation, which utilize **several gaussian kernel** with **pre-defined parameters** extracted from **raw BCG** to synthesize the **unaffected BCG signals**

$$\theta_i, a_i, b_i = \min_{\theta_i, a_i, b_i} ||x(t) - z(t)||_2^2$$

Methodology——Features extraction

Fiducial Points (H, I, J, K, L, M, N)

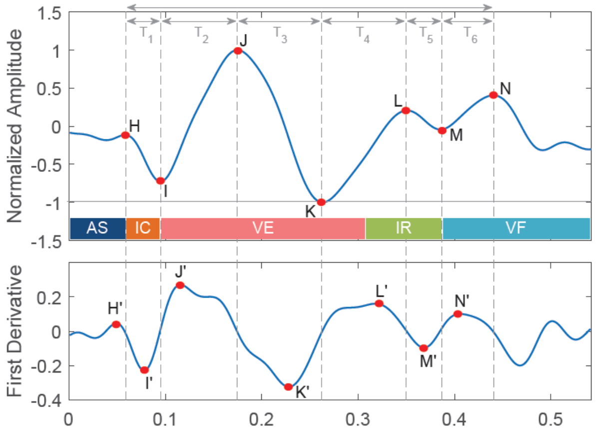

Table 1. The definition of fiducial features based on fiducial-point delineation.

Feature Type	Feature Name	Description
Time Interval	DU=T(H, N), T(H, I), T(I, J), T(J, K), T(K, L), T(L, M), T(M, N) T(H', I'), T(I', J'), T(J', K'), T(K', L'), T(L', M'), T(M', N')	Time interval between each two consecutive fiducial points
Time Ratio	T(H, I)/DU, T(I, J)/DU, T(J, K)/DU, T(K, L)/DU, T(L, M)/DU, T(M, N)/DU	Ratios of section to whole cycle
Extremum	A(H), A(I), A(J), A(K), A(L), A(M), A(N) A(H'), A(I'), A(J'), A(K'), A(L'), A(M'), A(N')	Peak values of fiducial points
Displacement	|A(H)-A(I)|, |A(I)-A(J)|, |A(J)-A(K)|, |A(K)-A(L)|, |A(L)-A(M)|, |A(M)-A(N)|	Differences between Y-axis of points
Area Under Curve	AUC(H, I), AUC(I, J), AUC(J, K), AUC(K, L), AUC(L, M), AUC(M,N)	Area enclosed by $S_{bcg}(a, b)$ and $Y = min(S_{bcg})$

Methodology——User Authentication Model

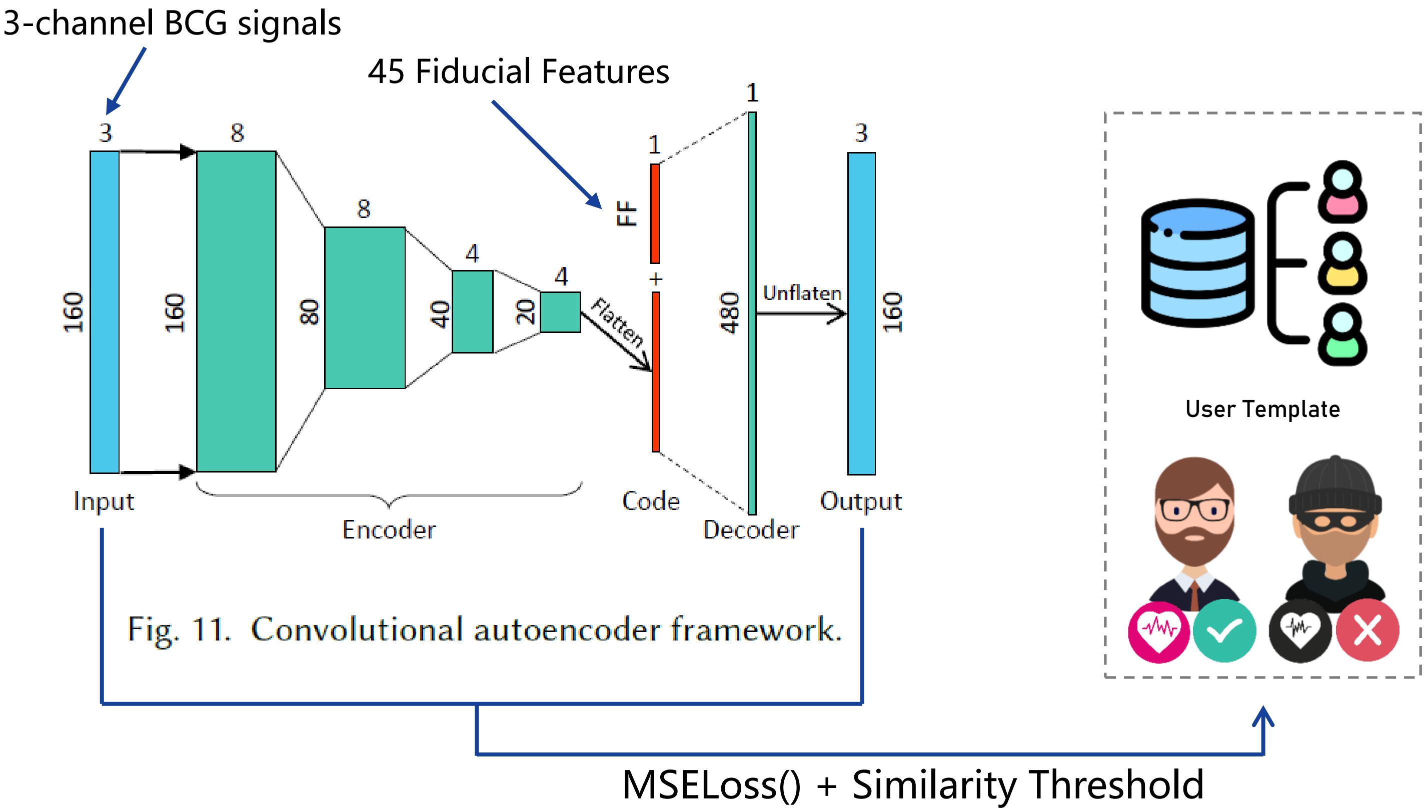

Fig. 11. Convolutional autoencoder framework.

Evaluation——Setup

Murata 3-axis accelerometer
SCA3300-D01

105 healthy subjects
(32 females, age 18-57)

Procedure

- **105 subjects** are asked to sit still and recline against the chair's back for **5 minutes**.
- **10 of them** evaluate the system's robustness (motion artifacts, sitting posture, heart rate, emotion, etc.)

Evaluation

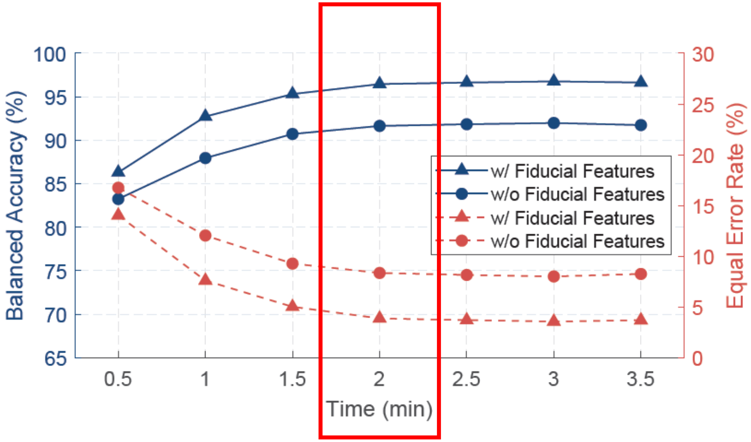

Fig. 12. Impact of the HCT for model initialization.

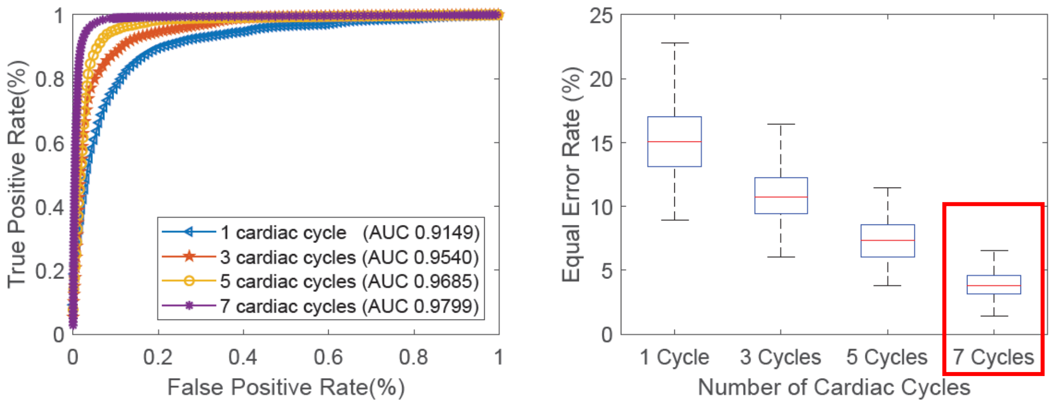

(a) ROC (b) EER

Fig. 13. ROC curves and EER with different number of cardiac cycles.

When heartprint collection time (HCT) = 2 minutes, and number of input cardiac cycles = 7

NF-Heart can verify users with a balanced accuracy (BAC) of 96.5% and an equal error rate (EER) of 3.8%

Evaluation

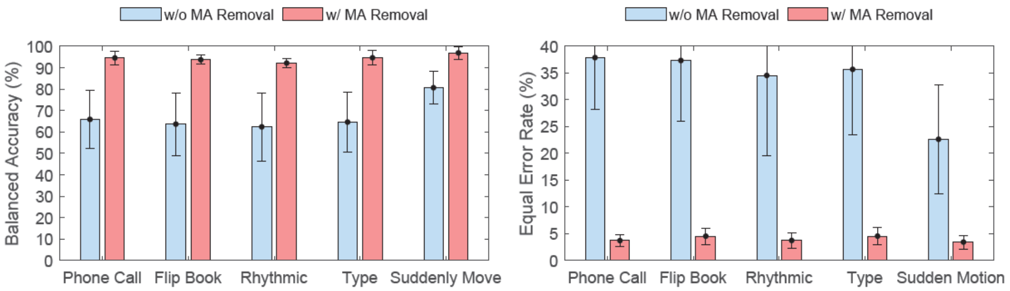

(a) BAC (a) EER

Fig. 14. The effectiveness of the two-stage MA removal.

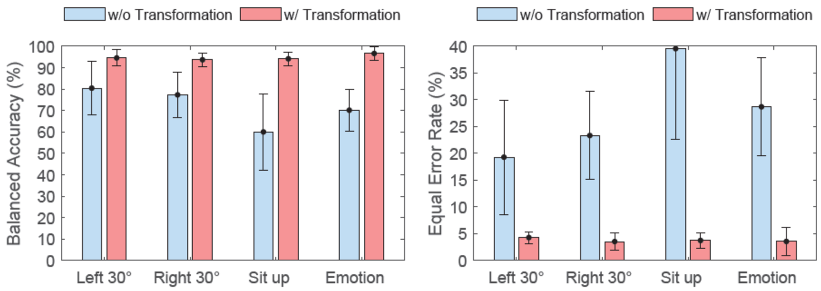

(a) BAC (b) EER

Fig. 15. The effectiveness of transformation.

- **MA removal** algorithm increases the **BAC by 27%** and reduces the **EER by 30%** on average
- **Transformation** scheme increases the BAC **by 23%** and reduces **the EER by 24%** on average
- The signal-processing pipeline makes NF-Heart resilient to various practical situations

Conclusion

- We propose a **near-field continuous user authentication system** using **unique BCG biometrics**. Our system can guarantee the **remote access security** of organizations by continuously verifying the identity of work-at-home staff.
- Compared to SOTA ECG or PPG-based CA scheme, **NF-Heart does not require wearables or direct contact with sensor nodes**.
- We design **multiple stages of signal processing** to recover distorted BCG signals for practical authentication in actual situations. **45 user-invariant fiducial features** are successfully extracted from BCG signals using refined U-net architecture, and the authentication is achieved with lightweight CAE framework.
- We design **a smart chair** for non-contact BCG measurements. We conduct extensive experiments involving **105 subjects** to validate the security, availability, and robustness of NF-Heart.

Thank You

香港科技大學
THE HONG KONG
UNIVERSITY OF SCIENCE
AND TECHNOLOGY

Yandao Huang
www.yandaohuang.cn

Principle of NF-Heart

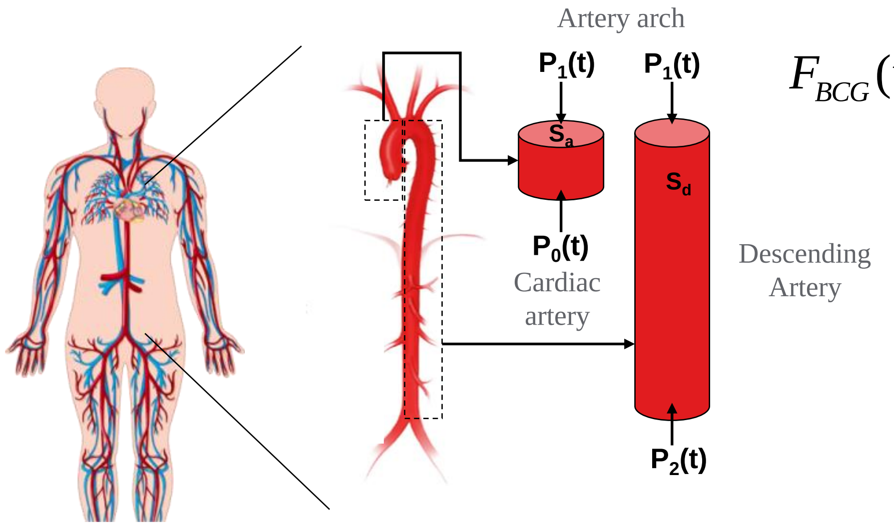

(a) Vascular tree of body

(b) Aorta tubes for BCG genesis model

Descending Aorta Pressure Gradients

Ascending Aorta Pressure Gradients

$$F_{BCG}(t) = S_d[P_1(t) - P_2(t)] - S_a[P_0(t) - P_1(t)]$$

Key insight: **BCG** measures body's micro-movements produced by the **recoil force** of the body in reaction to the cardiac ejection of blood, and **we can infer cardiac biometrics from BCG signals**.

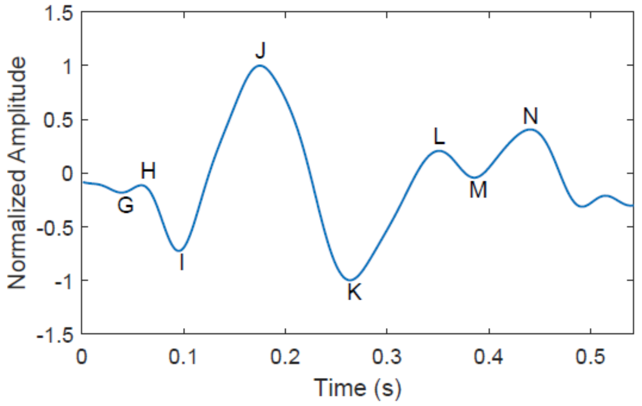

BCG wave complex
(G, H, I, J, K, L, M, N)

Principle of NF-Heart

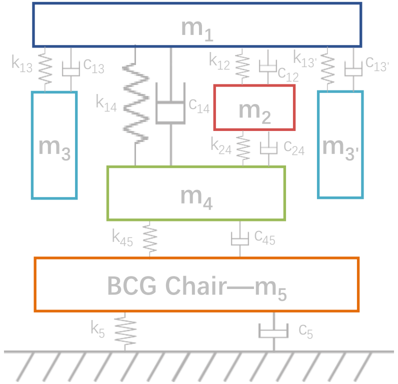

6-DoF spring-mass-damper model

m_1: upper torso

m_2: internal organs

m_3&$m_{3'}$: upper limbs

m_4: lower limbs

m_5: External chair

k: spring coeff.

c: damping coeff.

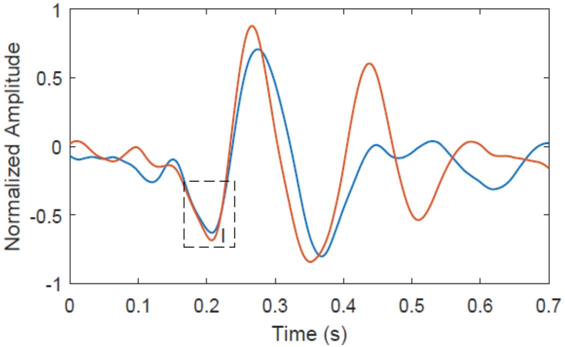

Distinctness of BCG waveform

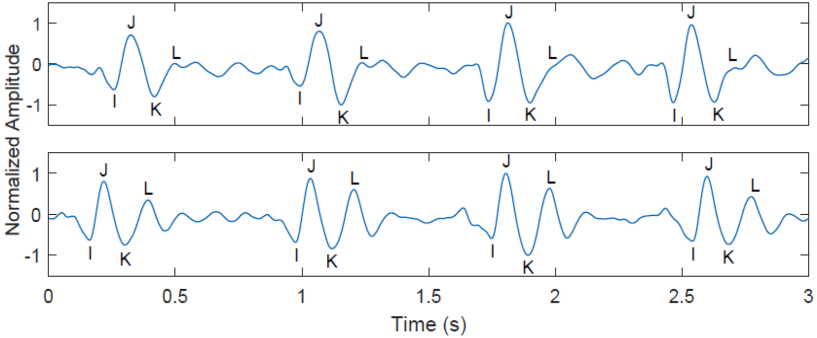

Consistency of BCG waveform

Advantages of BCG Biometrics

- Present in all living people
- Distinguishable across subjects
- Non-volitional
- Hard to hide
- Hard to forge
- Non-contact measurement

Methodology——Transformation

BCG dynamical model for eliminating effects of respiration, sitting posture, and user emotion.

$$
\begin{cases}
\dot{x} = \gamma x - \omega y \\
\dot{y} = \gamma x - \omega y \\
\dot{z} = -\sum\limits_{i\in\{H,I,J,K,L,M,N\}} a_i \Delta\theta_i \exp\left(-\dfrac{\Delta\theta_i^2}{2b_i^2}\right) - (z - z_0)
\end{cases}
$$

Integration

Fourth-order Runge–Kutta

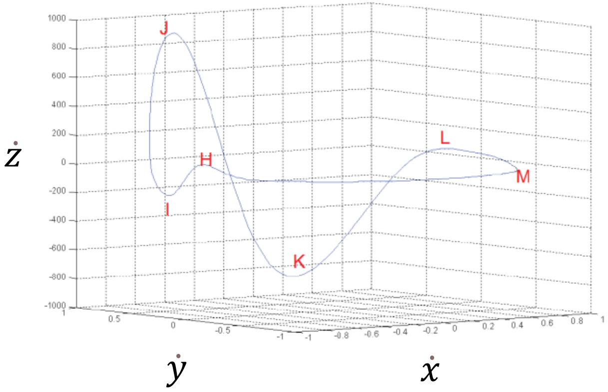

Three-dimensional display of single cycle BCG signals

where

$$\gamma = 1 - \sqrt{x^2 + y^2}$$

ω: angular velocity, related to the beat-to-beat heart rate as $\omega = 2\pi f_1$.

$z_0 = A\sin(2\pi f_2 t)$ The baseline wander of a BCG caused by respiration

We proposed the **BCG dynamical model** for transformation, which utilize **several gaussian kernel** with **pre-defined parameters** extracted from **raw BCG** to synthesize the **unaffected BCG signals**

$$\theta_i, a_i, b_i = \min_{\theta_i, a_i, b_i} \|x(t) - z(t)\|_2^2$$